https://doi.org/10.5194/egusphere-2025-1842
Preprint. Discussion started: 25 June 2025

Seismo-acoustic and GNSS monitoring of a record-breaking storm in the Black Sea: Evidence of climate change and intensifying natural hazards

Laura Petrescu[1,2,*], Bogdan Antonescu[1,2], Sorin Nistor[3], Iustin Floroiu[4,5], Dragoș Ene[1], Daniela Ghica[1], Constantin Ionescu[1], Andrei Anghel[4], Mihai Datcu[4]

1. National Institute for Earth Physics, Magurele, Romania
2. University of Bucharest, Faculty of Physics, Magurele, Romania
3. University of Oradea, Faculty of Construction, Cadaster and Architecture, Oradea, Romania
4. Politehnica University of Bucharest, Faculty of Electronics, Telecommunications and Information Technology, Bucharest, Romania
5. Politehnica University of Bucharest, Doctoral School of Electronics, Telecommunications & Information Technology, Bucharest, Romania

* laura.petrescu@infp.ro

Abstract

In August 2024, a devastating storm struck Romania's Black Sea coast, setting new precipitation records and highlighting the increasing frequency of extreme weather events. This study explores the integration of non-conventional sensors (seismic, GNSS, infrasound, and satellite data) with ERA5 meteorological reanalysis to monitor storm dynamics. High-frequency (>30 Hz) seismic signals captured precipitation, while microseismic bands (0.1-1Hz) reflected wave-induced ground motion. Infrasound data, analyzed using unsupervised learning, revealed distinct storm phases and showed strong spectral correlation with recorded ground motion, pointing to coupled atmosphere-lithosphere processes induced by the storm. The infrasound array also detected over 1,100 signals in the 0.6-7 Hz band, matching lightning discharges observed by geostationary satellites. GNSS-derived estimates of precipitable water vapor tracked atmospheric moisture buildup and showed clear correlation with intense rainfall, including potential precursory signals days before peak precipitation. This study highlights the value of integrating diverse, non-traditional datasets to enhance the resolution and depth of storm analysis. Their combined use offers a more holistic understanding of storm evolution and supports the development of improved early-warning systems in vulnerable coastal regions.

Graphical abstract

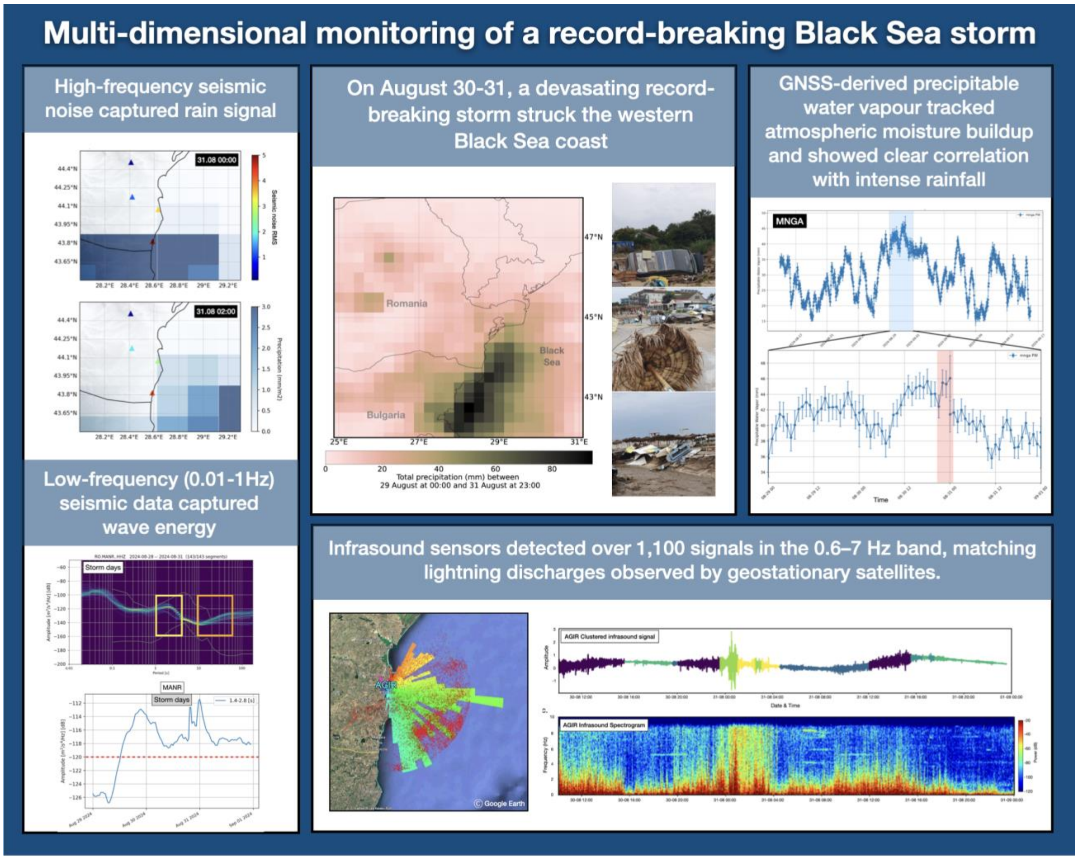

Multi-dimensional monitoring of a record-breaking Black Sea storm

High-frequency seismic noise captured rain signal

On August 30-31, a devasating record-breaking storm struck the western Black Sea coast

GNSS-derived precipitable water vapour tracked atmospheric moisture buildup and showed clear correlation with intense rainfall

Low-frequency (0.01-1 Hz) seismic data captured wave energy

Infrasound sensors detected over 1,100 signals in the 0.6–7 Hz band, matching lightning discharges observed by geostationary satellites.

https://doi.org/10.5194/egusphere-2025-1842
Preprint. Discussion started: 25 June 2025

1. Introduction

Climate change has become a critical global issue, with far-reaching effects on weather patterns and the frequency and intensity of extreme events (Stott, 2016). These changes are not only contributing to more severe weather events but also altering the timing, location, and duration of storms, making them harder to predict and manage (Bengtsson et al., 2006). Understanding how to effectively monitor and predict the behavior of storms, particularly extreme ones, is crucial for improving forecasting models, enhancing early warning systems, and mitigating their impacts on both natural and human systems.

Traditional meteorological monitoring relies heavily on ground-based stations, weather radars, and satellite observations to track and predict storm behavior (Kober and Tafferner, 2009). These systems have been the backbone of weather forecasting for decades, providing valuable data on temperature, pressure, wind speed, and precipitation. However, while these methods are effective, they often have limitations in terms of spatial coverage (e.g. Sokol et al., 2021), particularly in remote or hard-to-reach areas. Additionally, they may struggle to capture certain atmospheric phenomena in real-time. As a result, non-conventional monitoring methods are increasingly being integrated into storm tracking efforts to complement existing meteorological approaches (e.g. Bosy et al., 2012; Burtin et al., 2016; Diaz et al., 2023; Coviello et al., 2024) .

In this context, our study focuses on the integration of alternative environmental datasets, including GNSS stations, infrasound sensors, and seismic data, to track the dynamics of an extreme storm event, as part of a national climate change resilience strategy, implemented through the DTE Climate project (https://dteclimate.upb.ro/). GNSS data provide valuable information on atmospheric water vapor, helping to track moisture changes that influence storm formation and intensity (Bosy et al, 2012; Marut et al., 2022). Infrasound sensors detect low-frequency acoustic waves generated by storm activity, such as lightning or large-scale weather system movements like microbaroms (e.g. Landès et al., 2012). Seismic data, though traditionally used for earthquake monitoring, can also record vibrations caused by storm-induced pressure changes, making it useful for detecting rainstorms, floods, or tropical cyclones (e.g. Retailleau and Gualtieri, 2021). Through the integration of these diverse sensor networks, our work highlights their synergy in improving storm detection, monitoring capabilities, and early warning systems, contributing to more robust climate resilience strategies.

2. Study area and storm overview

The Black Sea region (Figure 1) is characterized by a unique combination of geographic and meteorological features that significantly influence its climate and weather patterns. Nestled between Europe and Asia, the Black Sea is bordered by six countries with diverse landscapes, from mountainous areas to flat plains. This geography, combined with the Black Sea's relatively shallow waters compared to oceanic environments and its connection to the Mediterranean through the Bosphorus Strait, creates an environment where rapid changes in weather are common. Understanding the dynamics of these extreme weather events is crucial, as they can have a profound impact on the environment, economy, and daily life in the region. Monitoring such events is key to improving our ability to predict their occurrence and intensity. By studying the complex atmospheric processes that govern these storms, we can enhance predictive models and refine early warning systems, ultimately helping to mitigate the risks and protect the communities and ecosystems most vulnerable to these extreme weather phenomena.

https://doi.org/10.5194/egusphere-2025-1842
Preprint. Discussion started: 25 June 2025

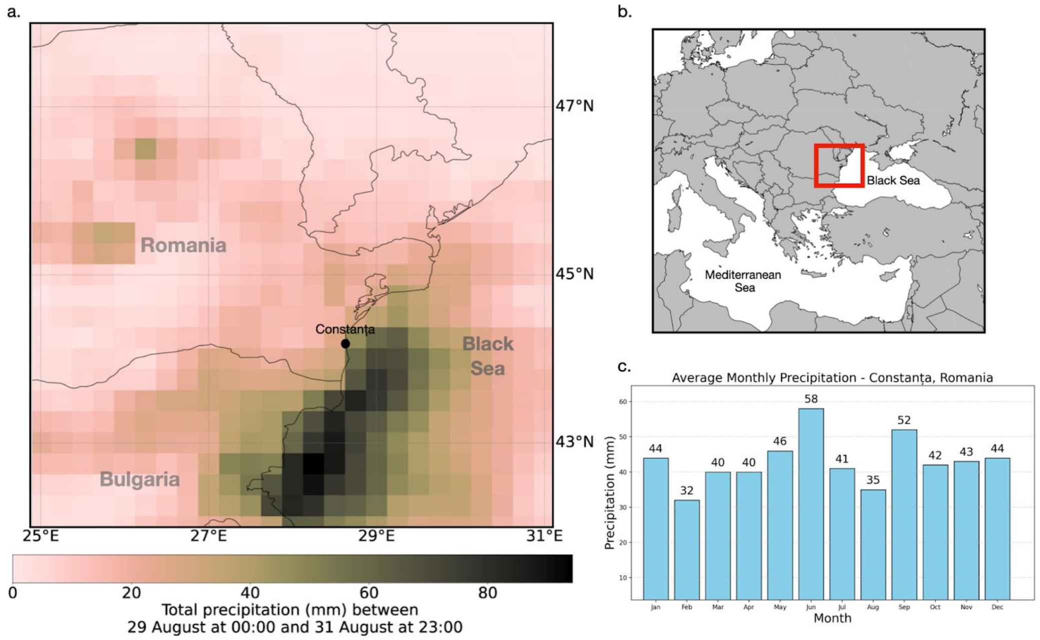

Figure 1. a. Total precipitation accumulated (in mm, shaded according to the scale) between 29 August 00 UTC and 31 August 23:00 UTC extracted from ERA5 data. The positions of the seismic stations in eastern Romania are also indicated; b. Map of Europe with red square marking the study region; c. Average monthly precipitation rates in Constanța, Romania.

In August 2024, Romania experienced severe flooding, largely driven by a storm that brought unusual precipitation patterns to the Black Sea coastal region. Exceptional precipitation totals were recorded over south-eastern Romania in Mangalia (225.9 mm), Agigea (145 mm), and Tuzla (118 mm), leading to significant flooding in coastal towns (Figure 1). Over 800 emergency calls prompted large-scale intervention by ISU Dobrogea, focusing on evacuations, debris clearance, and infrastructure restoration (Antonescu et al. 2024).

An analysis conducted by ClimaMeter (www.climameter.org, Faranda et al. 2024, Antonescu et al. 2024) immediately after the event, showed that low pressure systems similar to the one that caused the floods typically result in reduced rainfall (7 mm day^{-1}, or up to 15% less) in eastern Romania compared to historical trends. However, this particular storm led to a significant local increase in precipitation, particularly in Constanța, one of the coastal cities severely affected by the flooding. In Constanța, daily rainfall reached up to 5 mm day^{-1}, or up to 10% more than usual, marking a notable deviation from the region's typical weather behavior. The changes in precipitation that contributed to the flooding are largely attributed to human-induced climate change, with natural climate variability likely playing a modest role. As climate change continues to influence weather patterns, understanding the connection between changing precipitation levels and extreme weather events like flooding is crucial for improving forecasting and resilience in the face of such disasters.

https://doi.org/10.5194/egusphere-2025-1842
Preprint. Discussion started: 25 June 2025

3. Data and Methods

The analysis of the storm event integrates a variety of data sources and methodologies to provide a comprehensive understanding of its dynamics. Seismic data, infrasound measurements, GNSS water vapor data, and ERA5 reanalysis data are all utilized to capture different aspects of the storm's behavior (Figure 2). Seismic data offers insights into ground vibrations and atmospheric disturbances, while infrasound monitoring detects low-frequency acoustic signals generated by lightning and other meteorological phenomena. GNSS water vapor data provides valuable information on atmospheric moisture. Additionally, ERA5 reanalysis data (Hersbach et al. 2020), which provides detailed atmospheric and wave dynamics data, helps contextualize the storm's impact within broader weather patterns. Together, these diverse data sources enable a multifaceted approach to studying the storm and its effects.

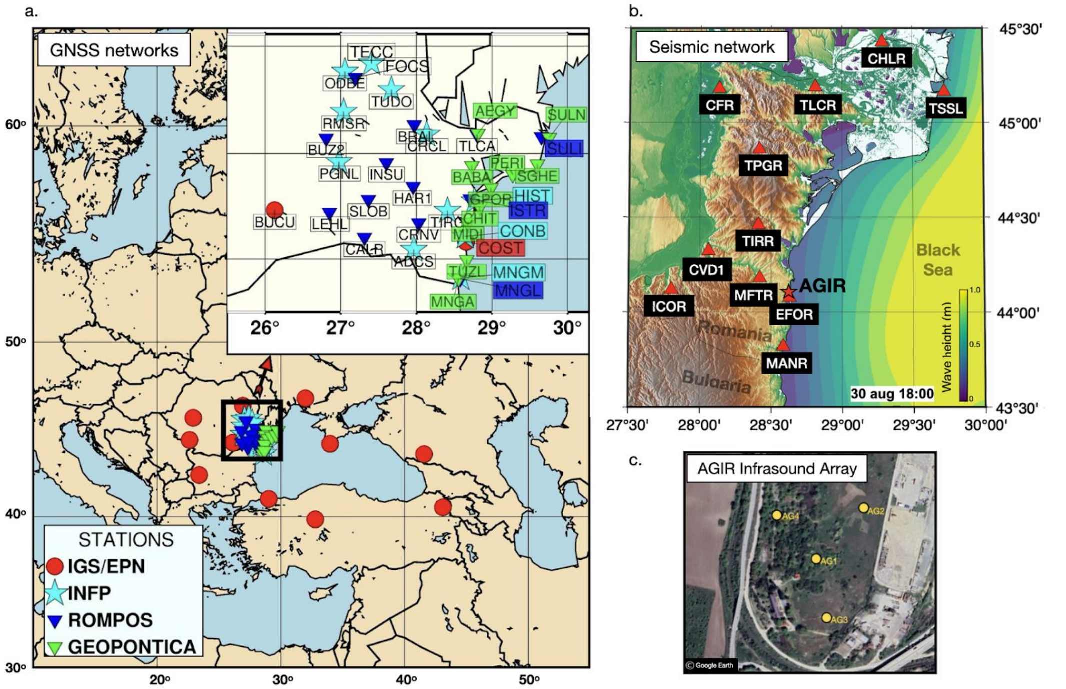

Figure 2. a. Map of Europe and the Black Sea coast showing GNSS stations and their belonging networks used for analysis in this study. b. Map of the Romanian sea coast showing seismic stations (red triangles) and the location of the AGIR infrasound array (star). Coloured contours represent total wave height at 18:00 on the 30th of August 2024 from ERA5 reanalysis data. c. The layout of the AGIR infrasound array.

3.1 Seismic Data

Seismic data represents vibrations of the Earth's surface, commonly referred to as seismic noise. These low-amplitude movements are recorded across the Earth's surface and are traditionally used to study the Earth's internal structure and detect earthquakes. Recently, it has increasingly found applications in meteorology and hydrology, particularly for monitoring weather events (e.g. Dias et al. 2023; Hua et al., 2023), destructive flood episodes (Burtin et al., 2016), ocean storms, and tropical cyclones (Gualtieri et al., 2018). Seismic noise can reveal the impact of atmospheric and oceanic conditions, providing valuable insights into weather events and climate changes (e.g. Bromirski etnal.l 2002; Aster et al, 2008; 2023). In particular, seismic data helps track variations in the Earth's surface caused by factors such as ocean waves, wind, and precipitation, offering a unique perspective on these phenomena (e.g. Grevemeyer et al., 2000; Borzì et al., 2022).

Seismic data also reveals two primary peaks (Figure 3) related to ocean wave interactions (Koper et al., 2015; Ardhuin et al., 2019; Tanimoto et al., 2023). The primary peak, observed in the range of 10–20 seconds (0.05–1 Hz), is generated by the impact of "swell" waves traveling in the same direction, inducing pressure variations in the Earth's crust that match the period of the waves. The secondary peak, in the range of 5–10 seconds (0.1–0.5 Hz), is produced by wind-driven waves, which propagate in different directions and generate pressure oscillations on the ocean floor (Ebeling et al., 2012). These seismic signals directly link ocean conditions with seismic activity (Li et al., 2020), providing insights into large-scale weather phenomena like ocean storms.

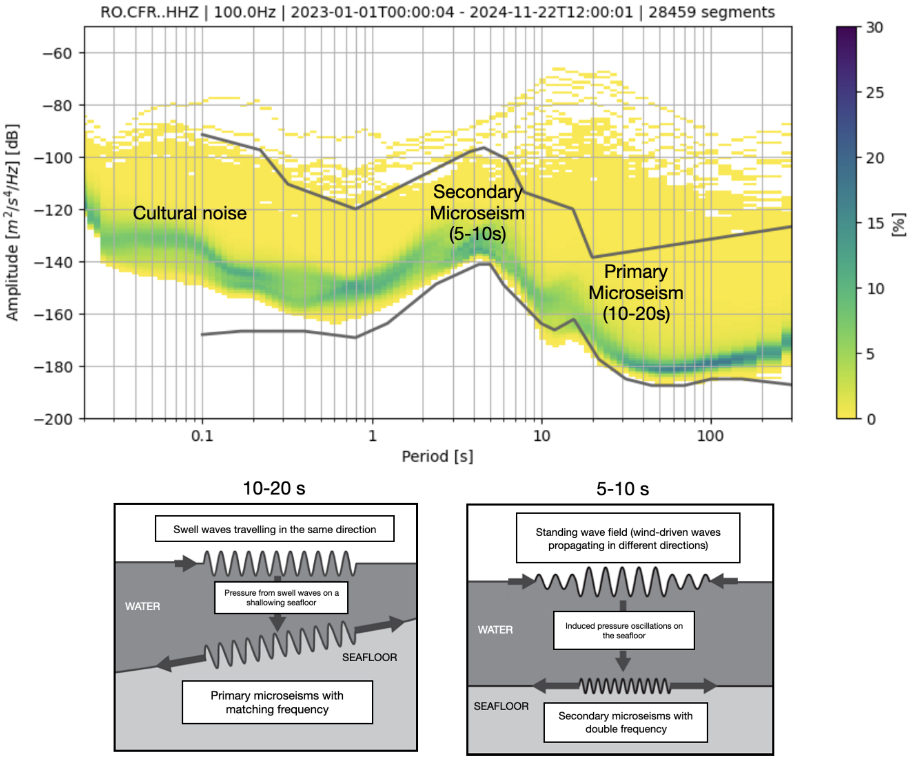

Figure 3. Probabilistic Power Spectral Density (PPSD) of seismic noise for station CFR, over two years, showing key sources of primary and secondary microseisms. Below, sketches illustrate the generation mechanisms: primary microseisms are caused by unidirectional swell waves inducing pressure fluctuations on a shoaling seafloor, while secondary microseisms result from nonlinear interactions of wind-driven waves over deeper water (modified after Ebeling, 2012).

Higher frequencies above 30 Hz are associated with the effects of precipitation and wind, as seen in studies like Rindraharisaona et al. (2022) or Diaz et al. (2023). These higher-frequency seismic signals help track more localized weather events, such as storms and heavy rainfall. Seismic data, when integrated with other meteorological tools, enhances the ability to monitor and predict weather events.

To analyse seismic data, the raw traces are first corrected for instrument response and converted to units of velocity. These are then filtered with butterworth filters adapted to capture the target signal: low pass filtering (<1 Hz) for wave-seafloor coupled interactions and high pass filtering (>30 Hz) to identify possible signatures of precipitation, essentially induced pressure fluctuations in the ground converted to weak seismic vibrations due to rain drops. Spectrograms of these filtered seismic traces are also used to visualise the potential signature of the two hydro-meteorological phenomena in the frequency content of ground vibrations.

Potential environmental signals in the seismic data were also investigated using power spectral density (PSD) analysis. To account for variations over time, a Probabilistic Power Spectral Density

https://doi.org/10.5194/egusphere-2025-1842
Preprint. Discussion started: 25 June 2025

(PPSD) method is applied. This approach combines PSD estimates from overlapping time windows into a probability distribution, providing a comprehensive view of the range and likelihood of noise levels at different frequencies. Typical noise conditions, as well as transient or extreme events, are captured in this analysis. To compute the PPSD, ObsPy was used (Beyreuther et al.,, 2010), which handles data gaps and ensures reliable normalization.

Temporal variations in PSD amplitudes are also analyzed to track changes in seismic noise at specific frequencies. By extracting PSD values at selected frequencies that are expected to capture primary and secondary microseisms, time series of noise levels are generated. These temporal PSDs allow for the identification of trends and correlations with environmental factors, such as ocean wave activity or weather conditions.

3.2 Acoustic Data

Infrasound waves are low-frequency acoustic waves that are inaudible to the human ear, typically below 20 Hz. These waves are generated by a variety of natural and anthropogenic sources, including meteorological events, volcanic eruptions, earthquakes, and human activities such as explosions and industrial processes (Campus, 2009; Bondár et al., 2022). In particular, infrasound is often associated with phenomena like thunderstorms, ocean waves, and large-scale atmospheric events, which generate pressure fluctuations that propagate through the atmosphere (e.g. Stopa et al., 2012; Landès et al., 2012; Listowski et al., 2022). These waves provide valuable information about the dynamics of weather systems (e.g. Hupe et al., 2019), making them an essential tool for monitoring and understanding environmental processes (e.g. Brachet et al., 2009; Hupe et al., *2022*).

For the monitoring of infrasound signals, we use data from an infrasound array system located at Eforie Nord-Agigea, Romania (AGIR, Figure 2). This array consists of multiple sensors, including SIS-1 infrasonic sensors (Seismowave), equipped with global positioning systems (GPS) and noise reduction technology.

To analyze the seismo-acoustic characteristics of the August 30–31 Black Sea storm, we used a two-pronged approach: (1) single-station signal analysis based on feature extraction and unsupervised machine learning, and (2) array-based analysis using classic multi-channel correlation algorithms. Together, these methods provide complementary insights into the acoustic behavior of the storm, capturing both local signal characteristics and spatial coherence across sensors.

For the single-station analysis, infrasound data recorded at the AGIR sensor (Figure 2) was segmented into 30-minute windows, and a set of time-frequency features was extracted to characterize the signal dynamics. These features describe how energy and frequency content evolve over time, providing insights into the signal's structure. The spectral centroid, spectral flux, spectral rolloff, and spectral entropy capture various aspects of the frequency distribution and its complexity, while the zero-crossing rate, mean, and variance of the power spectrum reflect signal activity and variability. These features together form a multidimensional representation of the infrasound signal during the storm.

The extracted features were used as input for K-Means clustering (MacQueen, 1967), an unsupervised machine learning algorithm that partitions data into a predefined number of groups, in this case, seven. K-Means minimizes within-cluster variance by iteratively assigning feature

https://doi.org/10.5194/egusphere-2025-1842
Preprint. Discussion started: 25 June 2025

vectors to the nearest cluster centroid and updating the centroids based on the grouped data. This clustering method enables the identification of distinct acoustic patterns in the signal (e.g. Pásztor et al., 2023), offering a data-driven way to segment the storm's infrasound profile without requiring prior labels or assumptions.

In parallel with the single-station analysis, we also applied the Progressive Multi-Channel Correlation (PMCC) method (Cansi and Le Pichon, 2008; Le Pichon et al., 2010) to detect and analyze coherent acoustic signals across an infrasound array. The PMCC method targets signals generated by atmospheric sources such as lightning or pressure disturbances, operating in the low-frequency range of 0.7 to 7 Hz. It is specifically suited for mini-array configurations, where signal coherence between closely spaced sensors can be exploited for precise signal detection and characterization.

The PMCC algorithm divides waveform recordings into overlapping time windows and processes them across logarithmically spaced frequency bands. Within each time-frequency segment, cross-correlations are computed between all sensor pairs to identify coherent wavefronts, signals that exhibit consistent arrival times across the array. From these detections, PMCC estimates several key propagation parameters, including back-azimuth (the direction of arrival), horizontal trace velocity, amplitude, duration, and dominant frequency. This approach is particularly effective in noisy environments and enables the discrimination of storm-generated infrasound from background signals or unrelated acoustic sources. The algorithm's output consists of a time-frequency map of signal detections enriched with physical metadata, allowing for detailed interpretation of the storm's acoustic footprint and its temporal evolution.

3.3 Satellite Observations

We also incorporated data from the Meteosat Third Generation (MTG) satellite system (Holmlund et al., 2021), specifically from its Lightning Imager (LI) sensor (Viticchie et al., 2020). The MTG satellites operate in geostationary orbit at approximately 36,000 km altitude, providing continuous observations over Europe, Africa, and surrounding waters. The Lightning Imager detects cloud-to-cloud, cloud-to-ground, and intra-cloud lightning flashes using four cameras that collectively cover 86% of the Earth's visible disc from the satellite's perspective.

For this study, we used Level 2 group data, which includes the geographical coordinates and timing of each detected flash. By mapping these detections, we were able to analyze the spatial distribution and temporal evolution of the storm's lightning activity. The dataset also offered insights into the storm's intensity and structure, complementing other meteorological observations.

3.4 GNSS Data

The use of GNSS technology for atmospheric monitoring provides a powerful tool for analyzing extreme weather events. Beyond its well-known applications in navigation and timing, GNSS has become a reliable method for sensing tropospheric water vapour, an essential driver of weather systems and a key variable in forecasting models (Guerova et al., 2016; Vaquero-Martínez and Antón, 2021). Over the past two decades, ground-based GNSS networks in Europe have contributed significantly to operational meteorology by providing near real-time estimates of atmospheric water vapour, aiding in the detection and tracking of severe weather, including heavy rainfall and storms (Karabatić et al., 2011; Priego et al., 2017; Jones et al., 2020). These high-resolution observations have proven valuable for both nowcasting and validating numerical weather prediction models (Wilgan et al., 2015; Bosy et al., 2012; Awange, 2012).

In this study, GNSS data were collected from several networks (Figure 2), including the International GNSS Service (IGS, Johnston et al., 2017), the EUREF Permanent Network (EPN, Bruyninx et al,, 2012), the Romanian Position Determination System (ROMPOS, Iliescu et al.., 2019), and GEOPONTICA (Dimitriu et al., 2017). A total of 37 permanent GNSS stations were analyzed over a 30-day period, with the rainiest interval selected at the midpoint of the study period. These stations provide high-quality, continuous observations critical for atmospheric monitoring.

The data were processed using a double-differenced, ionosphere-free combination of L1 and L2 carrier phases. This approach helps minimize errors such as ionospheric delays, satellite clock biases, and other common atmospheric effects. The resulting Zenith Tropospheric Delay (ZTD) values were then corrected using the Vienna Mapping Functions 3 (VMF3, Landskron et al., 2018), which improve the accuracy of ZTD by accounting for variations in the troposphere's atmospheric conditions. Once the ZTD was refined, it was converted into integrated precipitable water vapor (PWV) using surface meteorological data (temperature and pressure) from co-located weather stations, following the method outlined by Bosy et al. (2012). This process allowed for the derivation of high-resolution atmospheric water vapor content, critical for analyzing the dynamics of the extreme storm event over the Black Sea. By combining GNSS-derived PWV with data from other observational sources, the study captured the temporal and spatial variations in atmospheric moisture, offering valuable insights into the storm's development and intensity.

3.5 Meteorological Data

To compare the infrasound signals captured during the Black Sea extreme storm event, we extracted meteorological data from the open-access ERA5 reanalysis dataset, produced by the European Centre for Medium-Range Weather Forecasts (ECMWF). This dataset provides a comprehensive record of global weather conditions from 1950 to the present (Hersbach et al., 2023). ERA5 combines observational data and advanced numerical models to generate high-resolution atmospheric parameters, including precipitation (Figure 1), wind speed, and wave height.

For our study, the ERA5 data was used to track the meteorological context of the storm, offering insights into the intensity of precipitation, the evolution of wind patterns, and the development of oceanic wave heights. With high temporal (1 hour) and spatial (0.25° x 0.25°) resolution, ERA5 allows for a detailed comparison of the storm's meteorological characteristics over time. These comparisons help us understand the storm's dynamics and assess its impact, further enhancing the interpretation of infrasound signals and aiding in future storm prediction and monitoring efforts. The open-access nature of ERA5 ensures broad accessibility, contributing to the transparency and reproducibility of our storm analysis (Copernicus Climate Change Service, Climate Data Store, 2023).

4. Results

4.1 Seismic signatures of storm evolution

High frequency (>30 Hz) analysis of seismic noise reveals strong signals at times when high precipitation values were also recorded (Figure 4). Specifically, an example of the velocity envelope at station MANR and its spectrogram plotted for the period 29th of august at 12 AM (00:00) to 31st of August midnight UTC (Figures 4b,c) reveal strong signal around the 18:00 UTC - 00:00 UTC, when most precipitation was estimated in the grid cell of the station (more than 3 mm m^{-2}, Figure 4a). Similar signatures and precipitation-seismic spectrogram visualisations showed correlation with hourly precipitation levels, indicating that the high amplitude signal present on the high frequency velocity envelope and the time-frequency spectrogram at frequencies above 30 Hz is likely caused by rain. Previous research showed a correlation with rain drop size as well (Rindraharisaona et al., 2022), although we did not have access to such information.

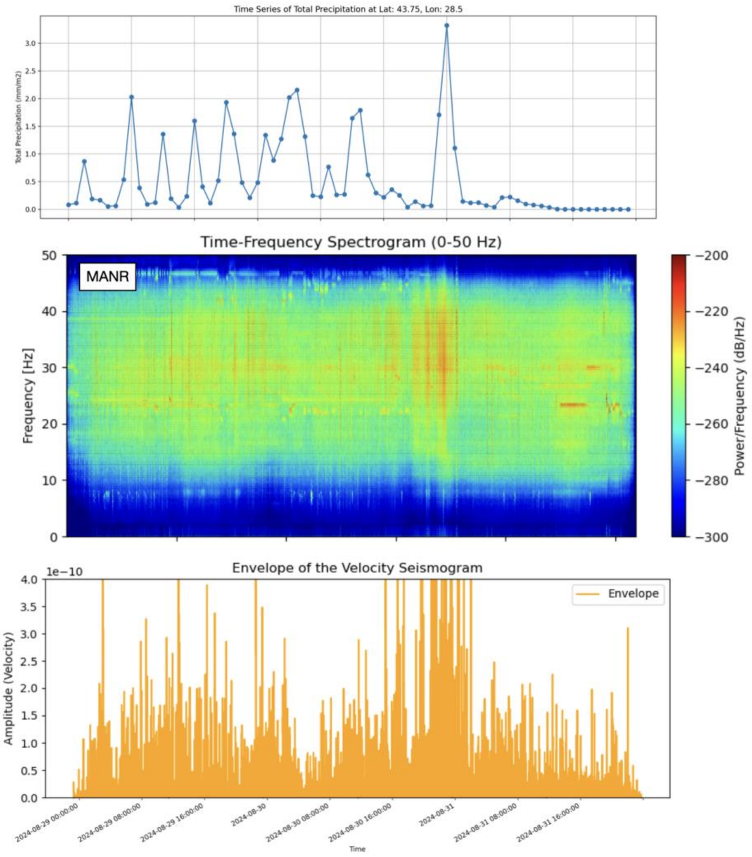

Figure 4. High frequency (30-50Hz) observations of the storm at station MANR. a. Tiem series of total precipitation per hour from ERA5 at the grid location of station MANR. b. Spectrogram of the velocity time series for station MANR. c. Envelope of the velocity seismogram at station MANR.

To visualise the signature of the storm passing over the network of broadband seismic stations in the coastal area, we also plotted the hourly precipitation values with the hourly root-mean-square amplitudes of the high-frequency (>30 Hz) seismic velocity envelopes recorded at seismic stations. Figure 5 shows three snapshots of hourly plots, illustrating a correlation between changing precipitation patterns from ERA5 data and the amplitudes of high-frequency seismic noise. This observation further supports the likelihood of a causal relationship.

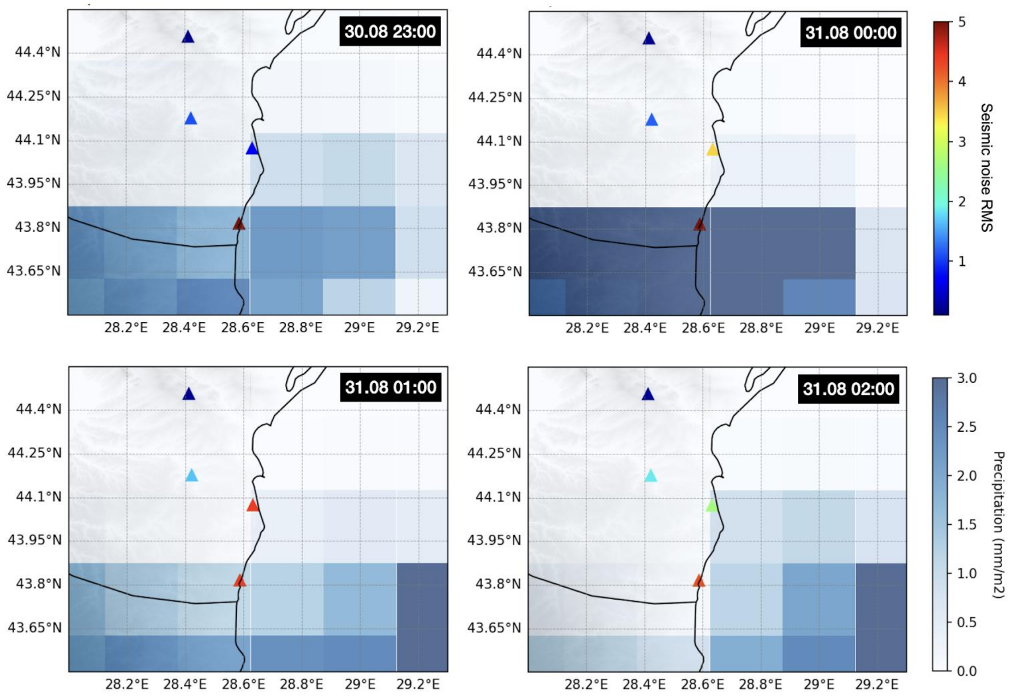

Figure 5. Distribution of hourly RMS of high pass filtered (>30 Hz) seismograms and precipitation data. Colours indicate hourly RMS amplitude of velocity envelopes filtered 30-50 Hz. Background coloured grid indicates the total precipitation (mm/m2) from ERA5 data.

The analysis of the microseismic noise frequency band is closely linked to the interaction between ocean waves and the seafloor, which is influenced by storm conditions. To assess the storm's impact, we analyze the PPSD (Probabilistic Power Spectral Density) of noise recorded at several stations during both storm and quiet days, using the latter as a baseline. Figure 6 shows examples of PPSD at stations MANR and MFTR (Figure 2), revealing differences in PSD amplitudes across the primary and secondary microseismic bands. These differences indicate the presence of high-intensity wind-driven waves and swell energy in the sea.

The secondary microseismic band shows a significant rise in amplitude during storms, driven by wind-induced pressure fluctuations in the shoaling seafloor (Figure 3, Ebeling et al., 2012). On quiet days, the PSD remains consistently lower, typically staying below the -120 dB threshold. This stark contrast emphasizes the role of atmospheric conditions in modulating seismic noise, with storms causing a notable increase in energy across both frequency bands. The temporal evolution of the PSD values (Figure 7) further highlights the storm's impact, with fluctuations corresponding to changes in environmental factors, reinforcing the connection between storm activity and the observed seismic signals.

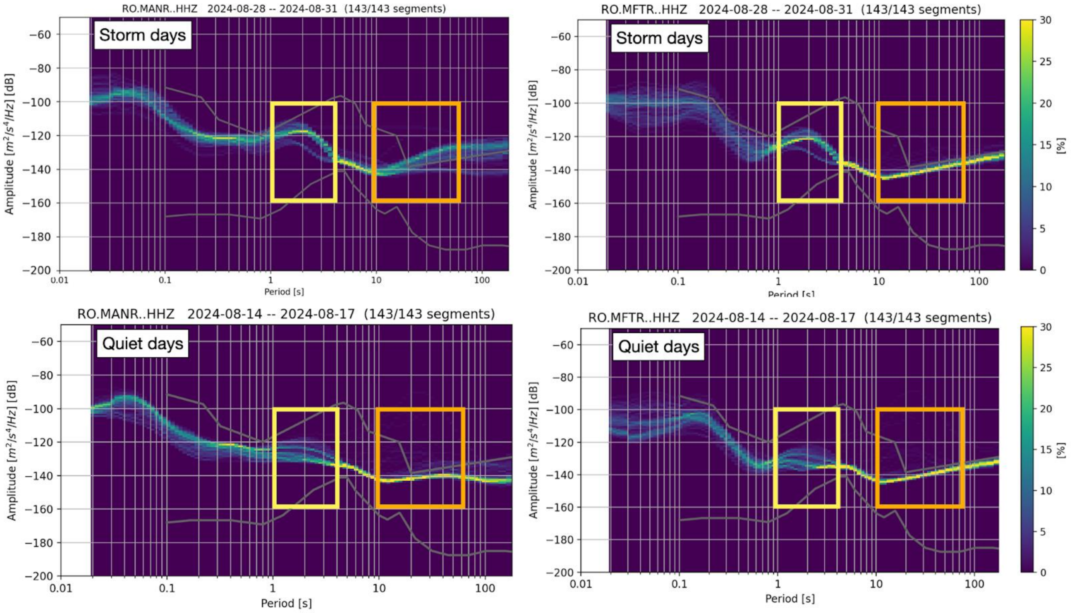

Figure 6. Probabilistic Power Spectral Density (PPSD) plots for two seismic stations near the Black Sea coast capturing the target storm signal in the microseismic bandwidths (marked with rectangles). The top panels show the PPSD distributions across frequencies, indicating the probability of power spectral density values in percentage for days including the Black Sea storm. The bottom panels show PPSD for days with no recorded events.

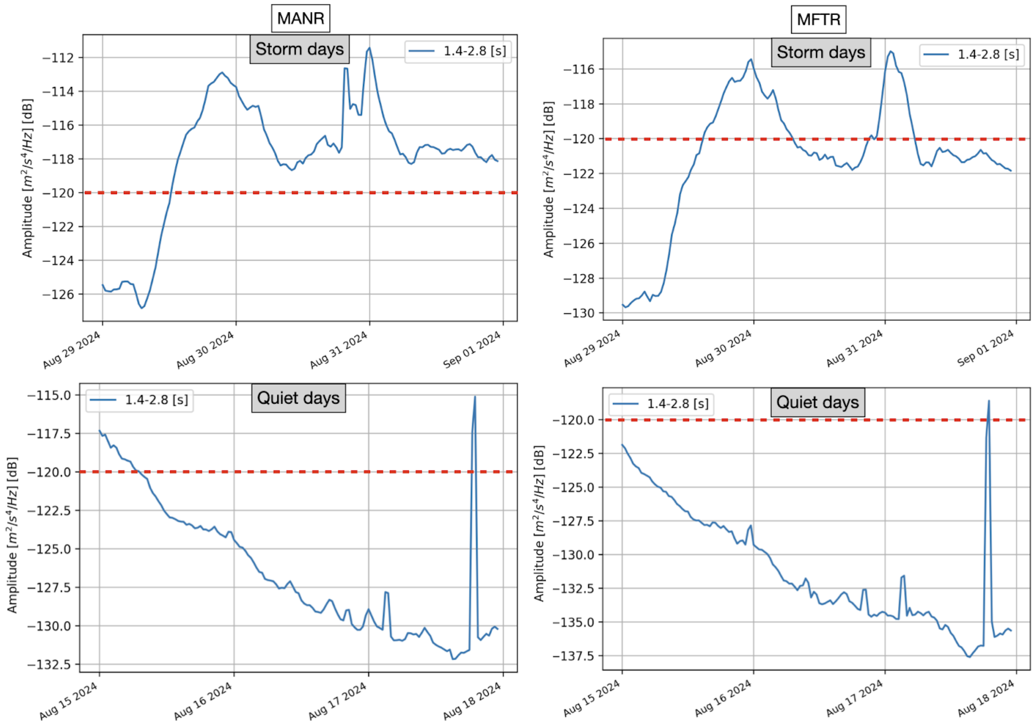

Figure 7. Temporal PSDs for two seismic stations near the Black Sea Coast in the secondary microseismic band showing significantly higher values (>-120 dB) during stormy days compared to days without recorded precipitation.

4.1 Infrasound and satellite lightning observations

4.1.1 Single station feature extraction

The evolution of time-frequency features over the duration of the Black Sea storm revealed distinct patterns in the infrasound signal (Figures 8 and 9). Most features, including spectral flux, spectral centroid, and spectral rolloff, exhibited a clear peak or a slightly bimodal peak corresponding to the storm's peak intensity, indicating a strong relationship between these features and the storm's dynamics. The peak in these features was most pronounced during the storm's active periods, reflecting rapid changes in the atmospheric conditions. However, the zero-crossings feature did not show a similarly distinct pattern, with its evolution being less evident in relation to the storm's phases. This suggests that most spectral features are sensitive to storm-related acoustic shifts.

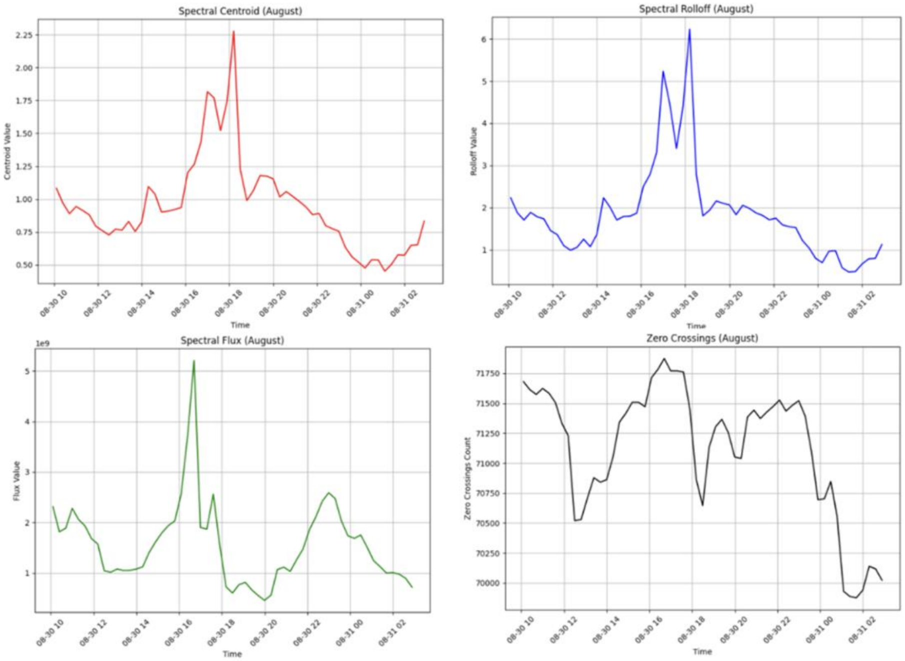

Figure 8. Time-frequency feature analysis for the single-station infrasound signal recorded at AGIR during the Black Sea Storm.

K-means clustering of the segmented infrasound signal, based on extracted time-frequency features, further revealed the relationship between the storm's acoustic dynamics and its temporal evolution, using 7 clusters for the enhancement of both detection of storm phases and event detection. The segmented signal highlighted distinct phases of the storm, with each segment corresponding to clusters representing specific changes in spectral content. These segments exhibited clear matches with the storm's progression, indicating that the clustering technique effectively tracked variations in storm intensity and the corresponding acoustic features. Interestingly, the spectral content of the infrasound signal showed similarities to seismic signal envelopes, particularly in the high frequency ranges (Figure 9), which may suggest a connection between the atmospheric pressure waves detected by infrasound and the ground vibrations captured by seismic instruments. This overlap implies that both seismic and infrasound signals could be complementary in capturing different aspects of storm dynamics, with seismic signals reflecting ground vibrations and infrasound capturing the atmospheric processes.

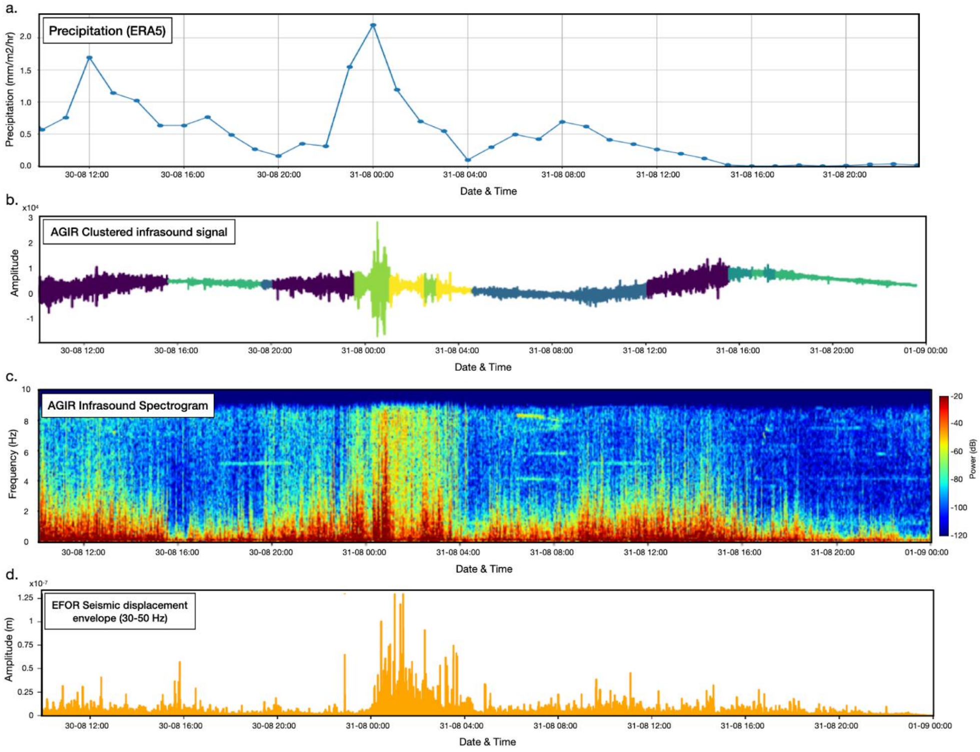

Figure 9. Clustering results of infrasound signals recorded at AGIR from the August Black Sea storm event compared with precipitation data and seismic signal from EFOR station. a. Average precipitation data from 1ºx1º around AGIR. b. Raw infrasound signal recorded at the AGIR sensor during the period of August 30–31, 2024, with different segments color-coded according to the cluster they belong to, based on K-means clustering of 30-minute time-frequency feature windows. c. The corresponding spectrogram generated using Blackman windowing with 128 samples and 70% overlap; d. Seismic displacement envelope at station EFOR, filtered between 30-50 Hz.

4.1.2 Array analysis and lightning detection

The PMCC algorithm allowed us to isolate coherent infrasound signals and estimate their propagation parameters, such as back-azimuth and arrival times, across the sensor network. These detections were cross-referenced with data from the MTG Lightning Imager, which recorded nearly 11,000 lightning strikes within a 50 km radius of the station during the Black Sea storm. The selected range ensured that the detected infrasound signals could be reliably linked to nearby lightning activity.

Approximately 1,100 infrasound detections were identified within the relevant frequency range of 0.6 to 7 Hz (Figure 10). These signals primarily consisted of long-duration wave trains, characterized by frequent amplitude peaks, likely associated with electrical discharges from lightning. The dominant frequency of these infrasound signals was approximately 3 Hz, with amplitudes varying between 0.01 and 3.4 Pa. These acoustic signatures, identified through the PMCC method, provide valuable insights into the storm's behavior, correlating infrasound signals with specific lightning events detected by the MTG Lightning Imager and enhancing our understanding of the atmospheric effects during the storm.

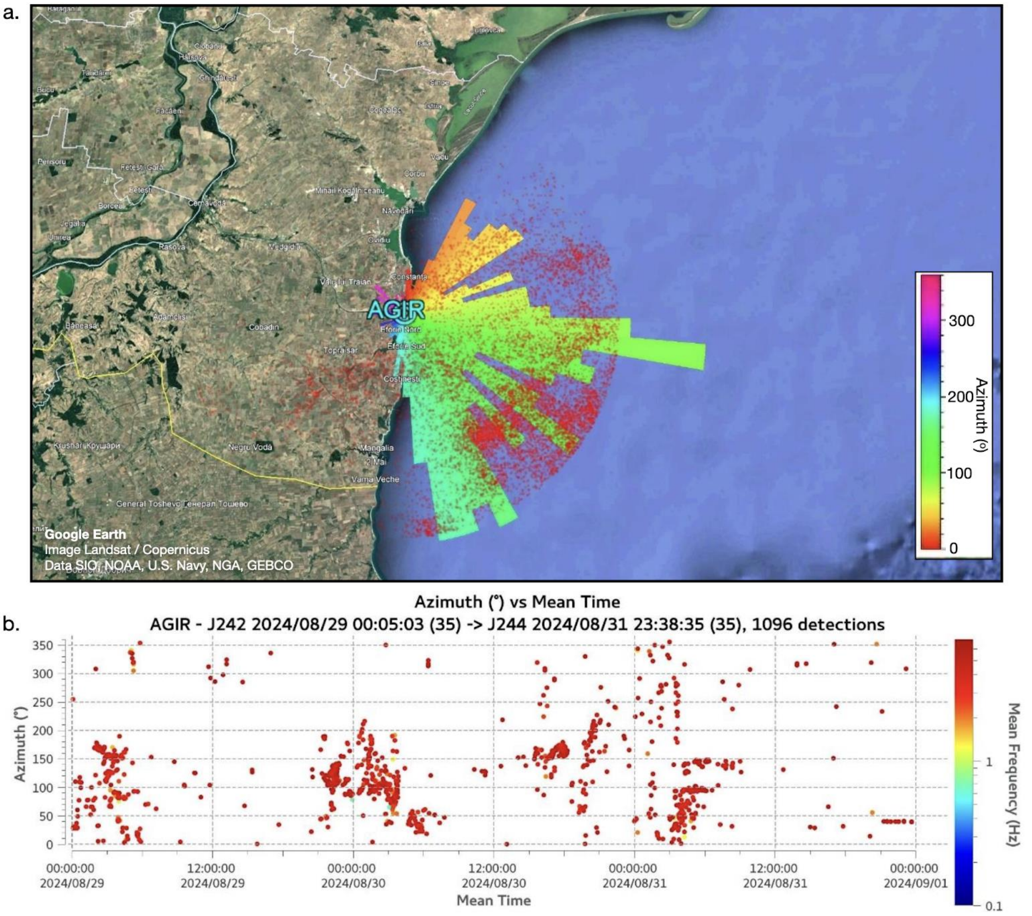

Figure 10. a. Polar histogram of infrasound detections from the AGIR station, displayed with © Google Earth, along with the locations of lightning strikes detected by the MTG Lightning Imager system for the period from August 29 to 31, 2024. The geographical position of the AGIR infrasound station is also shown on the map. b. diagram of high-frequency detections from the AGIR infrasound station between August 29 and 31, 2024.

4.4 GNSS-derived precipitable water vapor trends

The analysis of daily GNSS-derived precipitable water vapor (Figure 11) reveals clear temporal variations, with the highest PWV values consistently recorded on stormy days (>900 mm per day on DOY 240–243). Notably, the peak values occurred between DOY 241 and DOY 243 (Figure 11b), when the heaviest rainfall was observed (Figure 1). Coastal stations showed extremely high PWV values (>950 mm per day) compared to inland stations (>800 mm per day), with a slight decrease in PWV as we moved inland (Figure 11a). This spatial distribution highlights the geographical gradient of atmospheric moisture, with the highest PWV concentrations near coastal areas, decreasing gradually toward the north. Interestingly, some inland stations (BUCU, PGNL, RMSR) recorded their peak PWV on DOY 255, corresponding to the onset of the Boris storm, another significant extreme rainfall event that swept through Central and Eastern Europe (Athanase et al., 2024).

Elevated PWV was observed as early as DOY 239 (Figure 12a), suggesting that the tropospheric moisture loading began to increase several days before the onset of the rainfall. This accelerated increase in PWV can serve as an early indicator of a developing weather system. Remarkably, although HAR1, located inland, did not directly experience the extreme rainfall, it exhibited similar PWV behavior to coastal stations, suggesting that GNSS stations, even outside the immediate storm zones, can capture atmospheric signals indicative of intense precipitation. This finding offers a valuable precedent, showing that PWV measurements at GNSS stations not directly in the storm's path can still provide critical insights into moisture dynamics at the tropospheric level.

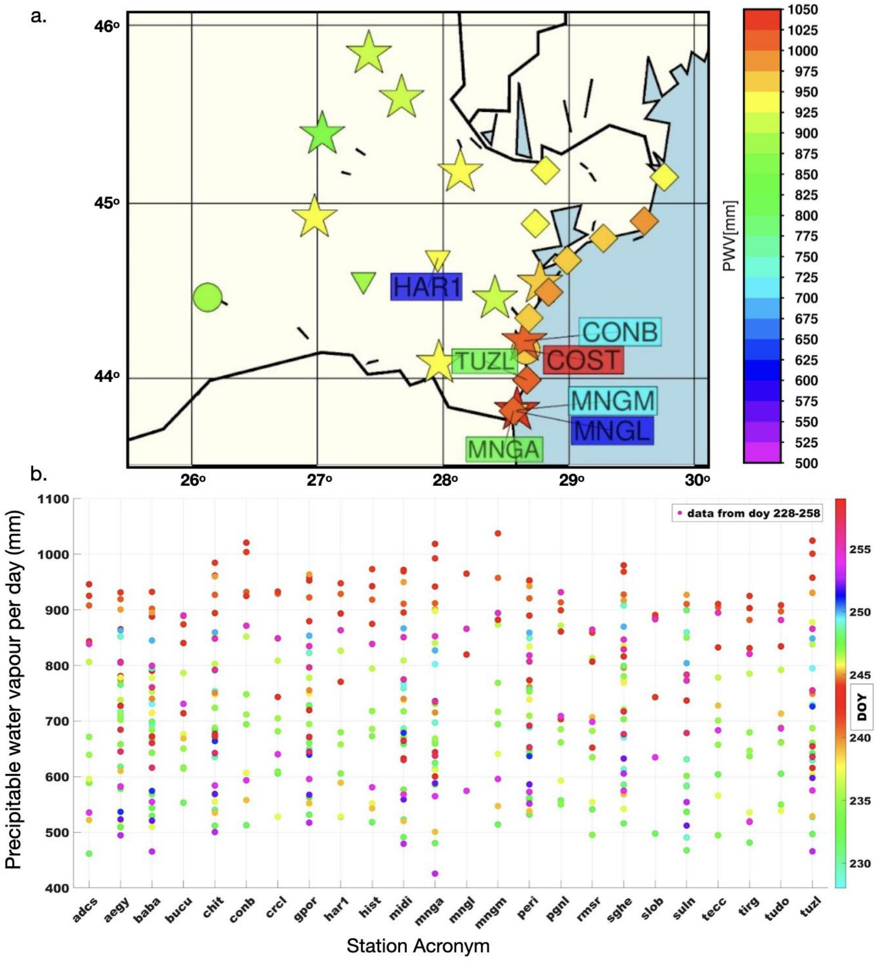

Figure 11. a: Map of GNSS stations coloured as a function of PWV estimated a day before the heavy rainfall in August 2024. b: Daily PWV values for each station showing the difference between rainy days (red circles) and non-rainy days (coloured as a function of Julian day index).

Shifting focus to hourly PWV data, Figure 12b shows the results from the MNGA station, which recorded the heaviest rainfall in the study area. Notably, MNGA also showed a rapid buildup of PWV, reaching values greater than 44 mm/hr just a few hours before the storm event. This rapid increase in PWV strongly suggests that the accumulation of atmospheric moisture is a precursor to extreme weather events, such as intense rainfall and storms. This observation aligns with known atmospheric dynamics, where a significant increase in water vapor content precedes heavy precipitation, providing further evidence of the potential for GNSS-based PWV monitoring to serve as an early warning tool for extreme weather.

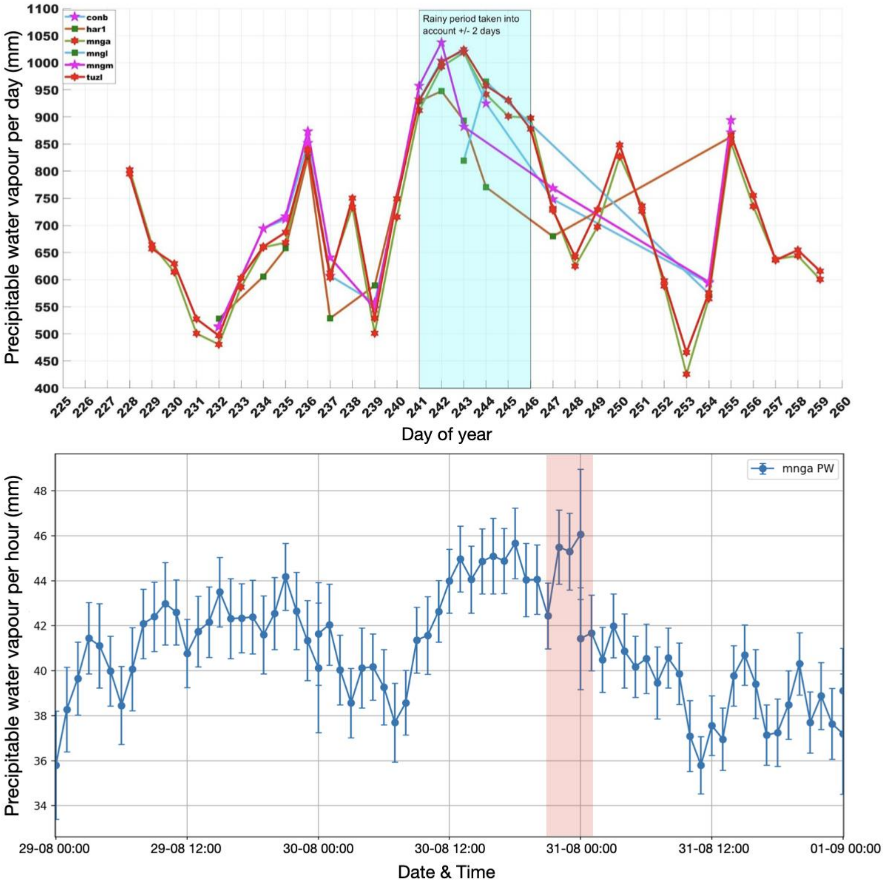

Figure 12. Time series of precipitable water vapour per day estimated at several GNSS stations (Figure 2), shown over the period of a month centered on the storm event (highlighted in blue); b. Hourly rates of PWV for station MNGA with the heaviest recorded rainfall at the location of the station, highlighted in blue.

5. Discussion

The integration of infrasound, seismic, and GNSS data in monitoring the extreme storm event over the Black Sea provides valuable insights into the dynamics of storm behavior and demonstrates the potential of non-conventional sensors for meteorological analysis. Infrasound data, for instance, revealed a clear acoustic signature of lightning activity, with signals detected in the range of 0.6 to 7 Hz corresponding to electrical discharges. The high frequency of infrasound detections (around 1,100) supports its utility as a reliable tool for tracking storm-related phenomena, particularly lightning, which is difficult to capture with traditional methods. However, the signals did not always perfectly align with lightning strikes, indicating that other factors, such as the movement of storm systems or variations in atmospheric conditions, may influence infrasound signatures. This suggests that refining the correlation between infrasound signals and lightning activity could be an avenue for future research, particularly in cases of sparse lightning or in remote regions.

A key aspect of the analysis was the use of unsupervised learning methods, such as K-means clustering, to identify patterns in the infrasound data. This approach segmented the infrasound signals into distinct clusters, suggesting the evolution of different phases of the storm. By identifying these phases, we can correlate shifts in spectral content with variations in storm intensity. However, a major goal for future work is to perform joint clustering with seismic data, which could provide a more comprehensive understanding of the storm's acoustic and seismic dynamics. Seismic data, particularly high-frequency seismic noise, closely resembled infrasound spectral decay, suggesting a coupling between the two types of signals. This spectral similarity may indicate that both infrasound and seismic signals are influenced by the same atmospheric and oceanic processes, such as pressure fluctuations caused by rainfall, wind, and storm-induced waves. The coupling between seismic and infrasound signals further emphasizes the need to integrate these data sources, as they capture different but complementary aspects of storm behavior. Future studies using joint clustering techniques will be crucial in enhancing the detection of storm phases and improving the understanding of the coupling between seismic and infrasound data.

Seismic data alone also showed a strong connection between high-frequency seismic noise and heavy rainfall, supporting previous studies that linked seismic signals to rainfall intensity. The distinction between high-frequency and low-frequency seismic noise is particularly noteworthy. High-frequency seismic noise correlated with precipitation, while low-frequency signals were associated with wave height and storm-driven winds. This suggests that different seismic frequencies capture distinct storm dynamics, with high-frequency signals reflecting localized rainfall impacts and low-frequency signals tied to broader atmospheric and oceanic interactions. This dual-frequency approach provides a more nuanced interpretation of seismic data in storm monitoring, highlighting its complexity.

The temporal variations observed in GNSS-derived integrated precipitable water vapor (PWV) provide valuable insights into atmospheric moisture dynamics before extreme weather events. The pronounced increase in PWV, particularly in the days leading up to and during the storm (DOY 241-243), supports the link between elevated atmospheric water vapor and precipitation. Notably, the buildup of PWV starting as early as DOY 239 suggests that rising moisture levels in the troposphere can serve as an early indicator of impending extreme rainfall. Even stations located up to 130 km inland, such as HAR1, recorded similar PWV trends, indicating that GNSS stations outside direct storm zones can still provide crucial atmospheric data. Hourly PWV trends further revealed a rapid increase several hours before precipitation, with values exceeding 44 mm/hr, highlighting the accumulation of moisture just before heavy rainfall. These findings align with the notion that increasing atmospheric moisture acts as a precursor to intense precipitation, highlighting the potential of GNSS-based PWV monitoring as a real-time tool for tracking moisture and understanding short-term atmospheric fluctuations.

The integration of GNSS, infrasound, and seismic data provides a more comprehensive understanding of storm dynamics than any single data source alone. The synergy between these diverse sensor types allows for the detection of atmospheric moisture, lightning activity, rainfall-induced seismic signals, and storm-driven oceanic interactions. Future research should focus on refining unsupervised learning algorithms for infrasound and seismic signal classification, optimizing joint clustering techniques, and improving the integration of these data sources to enhance storm forecasting and early-warning systems. We believe this multi-sensor approach holds promise for improving our ability to predict extreme weather events, understand their impacts, and mitigate associated risks.

6. Conclusions

This study presents a comprehensive analysis of a record-breaking storm over the Black Sea, using a combination of GNSS, infrasound, and seismic data to capture the dynamics of extreme weather events. Our findings underscore the power of multi-sensor networks in enhancing the understanding of storm behavior, particularly in the context of atmospheric moisture, lightning activity, and storm-induced seismic signals. GNSS-derived integrated precipitable water vapor (PWV) indicates a clear buildup of atmospheric moisture hours before the onset of heavy rainfall, providing valuable insights into the lead-up to extreme precipitation events. Infrasound and seismic data further complemented this analysis, with infrasound serving as a reliable tool for tracking lightning activity and seismic data revealing the link between rainfall intensity and high-frequency seismic noise.

The storm we analyzed is not only a significant meteorological event but also serves as a powerful example of how climate change may be influencing the frequency and intensity of extreme weather phenomena. Record-breaking storms like this are increasingly being recognized as evidence of shifting atmospheric conditions, driven by global climate change. The integration of GNSS, infrasound, and seismic data provides a more nuanced and holistic view of storm dynamics, highlighting the need for advanced monitoring systems to predict and respond to such extreme events. Moving forward, the combination of these innovative tools holds great potential for improving early-warning systems, enhancing storm forecasting, and better understanding the impacts of climate change on atmospheric and oceanic processes.

7. Code availability

Seismic data were processed with the open-source python framework for seismology Obspy (Beyreuther et al., 2010). Infrasound data was processed with the WinPMCC software (Le Pichon et al., 2010) developed by CEA/DASE (French Atomic Energy Commission, Environmental Assessment and Monitoring Department) and open-source Python libraries for signal processing. Some of the figures were made with GMT (Generic Mapping Tools, Wessel et al., 2019). The GNSS data was processed using Gamit/Globk (Herring et al., 2020) developed by Massachusetts Institute of Technology (http://www-gpsg.mit.edu/gg/).

8. Data availability

Seismic data are part of the Romanian National Seismic Network maintained by the National institute for Earth Physics (NIEP, www.infp.ro) and are freely available in the miniseed format via EIDA (European Integrated Data Archive, https://www.orfeus-eu.org/data/eida/). GNSS data are available for download from NIEP (http://gps.infp.ro/#/download) and are provided in the standardized RINEX v2 format, with 24-hour files sampled at 30-second intervals. Infrasound data at AGIR are available to download from NIEP via FDSN dataselect web service. Hourly hydro-meteorological data were obtained from the Copernicus Climate Change Service, Climate Data Store (https://doi.org/10.24381/cds.bd0915c6), ERA5 dataset (Hersbach et al., 2023). Lightning data came from Meteosat Third Generation Lightning Imager operated by EUMETSAT (The European Organisation for the Exploitation of Meteorological Satellites, https://www.eumetsat.int/).

9. Author contribution

Laura Petrescu: Conceptualization, Methodology, Software, Formal analysis, Data Curation, Writing-Original Draft, Visualization, Funding acquisition; **Bogdan Antonescu**: Conceptualization, Writing-Review & Editing, Visualization; **Sorin Nistor**: Software, Formal Analysis, Data curation, Visualisation, Writing-Review & Editing; **Iustin Floroiu**: Methodology, Software, Formal analysis, Data Curation, Writing-Original Draft, Visualization; **Dragoș Ene**: Software, Formal analysis, Data Curation, Writing-Review & Editing; **Daniela Ghica**: Software, Formal analysis, Data Curation; **Constantin Ionescu:** Funding Acquisition, Resources, Project administration; **Andrei Anghel:** Methodology, Supervision; **Mihai Datcu**: Methodology, Supervision, Funding Acquisition, Resources, Project administration.

10. Acknowledgments

We would like to thank the technicians and staff at NIEP for their support in installing, maintaining, and ensuring the proper functioning of the equipment used in this study. Additionally, we appreciate the efforts of those involved in data formatting and preparation (Cristian Neagoe, Eduard Nastase, Victorin Toader) which were essential for this work.

11. Financial support:

This work was carried out in the framework of the “Competence Center for Climate Change Digital Twin for Earth forecasts and societal redressment” Project PNRR- DTEClimate nr. 760008/31.12.2023, subproject Reactive “The Research center for climate change due to natural disasters and extreme weather events”, supported by the Ministry of Research, Innovation and Digitalization of Romania.

12. References

Antonescu, B., Dafis, S., & Faranda, D.: Changes in precipitation patterns driving August 2024 Romania floods mostly driven by human-driven climate change. *ClimaMeter, Institut Pierre Simon Laplace, CNRS*. https://doi.org/10.5281/zenodo.14056214, 2018.

Ardhuin, F., Gualtieri, L., Stutzmann, E., Nakata, N. and Fichtner, A.: Physics of ambient noise generation by ocean waves. In *Seismic ambient noise*, Eds: Nakata, N., Gualtieri, L., Fichtner, A. Cambridge University Press, 69-108, https://doi.org/10.1017/9781108264808.005, 2019.

Aster, R.C., McNamara, D.E. & Bromirski, P.D.: Multidecadal climate-induced variability in microseisms. *Seismological Research Letters*, 79(2), 194-202, https://doi.org/10.1785/gssrl.79.2.194, 2008.

Aster, R.C., Ringler, A.T., Anthony, R.E., & Lee, T.A.: Increasing ocean wave energy observed in Earth's seismic wavefield since the late 20th century. *Nature Communications*, 14(1), 6984, https://doi.org/10.1038/s41467-023-42673-w, 2023.

Athanase, M., Sánchez-Benítez, A., Monfort, E., Jung, T. and Goessling, H.F.: How climate change intensified storm Boris' extreme rainfall, revealed by near-real-time storylines. *Communications Earth & Environment*, *5*(1), 676, https://doi.org/10.1038/s43247-024-01847-0, 2024.

Awange, J.L.: Environmental monitoring using GNSS: Global navigation satellite systems, Springer, Heidelberg, https://doi.org/10.1007/978-3-540-88256-5, 2012.

Beyreuther, M., Barsch, R., Krischer, L., Megies, T., Behr, Y. and Wassermann, J.: ObsPy: A Python toolbox for seismology. *Seismological Research Letters*, *81*(3), 530-533, https://doi.org/10.1785/gssrl.81.3.530, 2010.

Bengtsson, L., Hodges, K.I. and Roeckner, E.: Storm tracks and climate change. *Journal of climate*, 19(15), 3518-3543, https://doi.org/10.1175/JCLI3815.1, 2006.

Bollinger, L., Perrier, F., Avouac, J.P., Sapkota, S., Gautam, U., Tiwari, D.R.: Seasonal modulation of seismicity in the Himalaya of Nepal, *Geophysical Research Letters*, 34(8), https://doi.org/10.1029/2006GL029192, 2007.

Bondár, I., Šindelářová, T., Ghica, D., Mitterbauer, U., Liashchuk, A., Baše, J., Chum, J., Czanik, C., Ionescu, C., Neagoe, C. and Pásztor, M.: Central and Eastern European Infrasound Network: contribution to infrasound monitoring, *Geophysical Journal International*, 230(1), 565-579, https://doi.org/10.1093/gji/ggac066, 2022.

Borzì, A.M., Minio, V., Cannavò, F., Cavallaro, A., D'Amico, S., Gauci, A., De Plaen, R., Lecocq, T., Nardone, G., Orasi, A., Picone, M., Cannata, A.: Monitoring extreme meteo-marine events in the Mediterranean area using the microseism (Medicane Apollo case study). *Scientific Reports*, 12(1), https://doi.org/10.1038/s41598-022-25395-9, 2022.

Bosy, J., Kaplon, J., Rohm, W., Sierny, J. and Hadas, T.: Near real-time estimation of water vapour in the troposphere using ground GNSS and the meteorological data, *Annales Geophysicae*, 30, 1379–1391, https://doi.org/10.5194/angeo-30-1379-2012, 2012.

Brachet, N., Brown, D., Le Bras, R., Cansi, Y., Mialle, P., Coyne, J.: Monitoring the Earth's Atmosphere with the Global IMS Infrasound Network, in: Infrasound Monitoring for Atmospheric Studies, edited by: Le Pichon, A., Blanc, E., Hauchecorne, A. , Springer, Dordrecht, https://doi.org/10.1007/978-1-4020-9508-5_3, 2010.

Bromirski, P.D. and Duennebier, F.K.: The near-coastal microseism spectrum: Spatial and temporal wave climate relationships. *Journal of Geophysical Research: Solid Earth*, 107(B8), ESE 5-1-ESE 5-20, https://doi.org/10.1029/2001JB000265, 2002.

Bruyninx, C., Habrich, H., Söhne, W., Kenyeres, A., Stangl, G. and Völksen, C.: Enhancement of the EUREF permanent network services and products, in: Proceedings of the International Association of Geodesy, *Symposium on Geodesy for Planet Earth, Buenos Aires, Argentina, 31 August-4 September 2009*, 27-34, 2012.

Burtin, A., Hovius, N. and Turowski, J.M.: Seismic monitoring of torrential and fluvial processes. *Earth Surface Dynamics*, 4(2), 285-307, https://doi.org/10.5194/esurf-4-285-2016, 2016.

Campus, P. and Christie, D.R.: Worldwide observations of infrasonic waves, in: Infrasound monitoring for atmospheric studies, edited by: Le Pichon, A., Blanc, E., Hauchecorne, A., Springer, Dordrecht, Netherlands, 185-234, https://doi.org/10.1007/978-1-4020-9508-5_6, 2009.

Cansi, Y. and Pichon, A.L.: Infrasound event detection using the progressive multi-channel correlation algorithm, in: *Handbook of signal processing in acoustics*., edited by: Havelock, D., Kuwano, S., Vorländer, M., Springer, New York, 1425-1435, https://doi.org/10.1007/978-0-387-30441-0_77, 2008.

Coviello, V., Palo, M., Adirosi, E. and Picozzi, M.: Seismic signature of an extreme hydro-meteorological event in Italy, *Natural Hazards*, 1(1), 17, https://doi.org/10.1038/s44304-024-00018-7, 2024.

Diaz, J., Ruiz, M., Udina, M., Polls, F., Martí, D., Bech, J.: Monitoring storm evolution using a high-density seismic network, *Scientific Reports*, 13(1), https://doi.org/10.1038/s41598-023-28902-8, 2023.

Dimitriu, R.G., Stanciu, I.M., Barbu M.-.B., Dobrev, N., Dumitru, P.: First results on the western Black Sea coast geodynamics resulted from GeoPontica permanent GNSS stations network data processing, in: Proceedings of the 17th International Multidisciplinary Scientific GeoConference SGEM, Albena, Bulgaria August 2017, 17(11), 149-157, 2017.

Ebeling, C.W.: Inferring Ocean Storm Characteristics from Ambient Seismic Noise. A Historical Perspective, *Advances in Geophysics*, 53, 1-33. https://doi.org/10.1016/B978-0-12-380938-4.00001-X, 2012.

Faranda, D., Messori, G., Coppola, E., Alberti, T., Vrac, M., Pons, F., Yiou, P., Saint Lu, M., Hisi, A. N. S., Brockmann, P., Dafis, S., Mengaldo, G., and Vautard, R.: ClimaMeter: contextualizing extreme weather in a changing climate, *Weather Climate Dynamics*, 5, 959–983, https://doi.org/10.5194/wcd-5-959-2024, 2024.

Grevemeyer, I., Herber, R. and Essen, H.H.: Microseismological evidence for a changing wave climate in the northeast Atlantic Ocean. *Nature*, 408(6810), 349-352, https://doi.org/10.1038/35042558, 2000.

Gualtieri, L., Camargo, S.J., Pascale, S., Pons, F.M.E., & Ekström, G.: The persistent signature of tropical cyclones in ambient seismic noise, *Earth and Planetary Science Letters*, 484, 287-294. https://doi.org/10.1016/j.epsl.2017.12.026, 2018.

Guerova, G., Jones, J., Douša, J., Dick, G., de Haan, S., Pottiaux, E., Bock, O., Pacione, R., Elgered, G., Vedel, H. and Bender, M.: Review of the state of the art and future prospects of the ground-based GNSS meteorology in Europe, Atmospheric Measurement Techniques, 9(11), 5385–5406, https://doi.org/10.5194/amt-9-5385-2016, 2016.

Herring, T., King, R., Floyd, M., McClusky, S.: GAMIT Reference Manual GPS Analysis at MIT Release 10.7. GAMIT/GLOBK, 2020.

Hersbach, H., Bell, B., Berrisford, P., Hirahara, S., Horányi, A., Muñoz-Sabater, J., Nicolas, J., Peubey, C., Radu, R., Schepers, D. and Simmons, A.: The ERA5 global reanalysis, *Quarterly Journal of the Royal Meteorological Society*, *146*(730), 1999-2049, 2020.

Hersbach, H., Bell, B., Berrisford, P., Biavati, G., Horányi, A., Muñoz Sabater, J., Nicolas, J., Peubey, C., Radu, R., Rozum, I., Schepers, D., Simmons, A., Soci, C., Dee, D., Thépaut, J-N.: ERA5 hourly data on single levels from 1940 to present. Copernicus Climate Change Service (C3S) Climate Data Store (CDS), https://doi.org/10.24381/cds.adbb2d47, 2023.

Holmlund, K., Grandell, J., Schmetz, J., Stuhlmann, R., Bojkov, B., Munro, R., Lekouara, M., Coppens, D., Viticchie, B., August, T. and Theodore, B.: Meteosat Third Generation (MTG): Continuation and innovation of observations from geostationary orbit, *Bulletin of the American Meteorological Society*, *102*(5), E990-E1015, https://doi.org/10.1175/BAMS-D-19-0304.1, 2021.

Hua, J., Wu, M., Mulholland, J.P., Neelin, J.D., Tsai, V.C. and Trugman, D.T.: High-resolution precipitation monitoring with a dense seismic nodal array. *Scientific Reports*, 13(1), 11450, https://doi.org/10.1038/s41598-023-38008-w, 2023.

Hupe, P., Ceranna, L., Pilger, C., de Carlo, M., Le Pichon, A., Kaifler, B. and Rapp, M.: Assessing middle atmosphere weather models using infrasound detections from microbaroms. *Geophysical Journal International*, 216(3), 1761-1767, https://doi.org/10.1093/gji/ggy520, 2019.

Hupe, P., Ceranna, L., Le Pichon, A., Matoza, R.S. and Mialle, P.: International Monitoring System infrasound data products for atmospheric studies and civilian applications. *Earth System Science Data Discussions*, 14, 4201–4230, https://doi.org/10.5194/essd-14-4201-2022, 2022.

Iliescu, A. I., Rus, T., Danciu, V., Moldoveanu, C., & Ilie, A.: Current situation of GNSS networks in Romania, *Bulletin of University of Agricultural Sciences and Veterinary Medicine Cluj-Napoca. Horticulture*, *76*(2), 2019.

Johnston, G., Riddell, A. and Hausler, G.: The international GNSS service, in: Springer handbook of global navigation satellite systems, edited by: Teunissen, P.J. and Montenbruck, O., Springer, Cham, Switzerland, 967-982, https://doi.org/10.1007/978-3-319-42928-1_33, 2017.

Jones, J., Guerova, G., Douša, J., Dick, G., de Haan, S., Pottiaux, E., Bock, O., Pacione, R. and Van Malderen, R.: Advanced GNSS tropospheric products for monitoring severe weather events and climate, COST Action ES1206 Final Action Dissemination Report, 563, 2020.

Karabatić, A., Weber, R. and Haiden, T.: Near real-time estimation of tropospheric water vapour content from ground based GNSS data and its potential contribution to weather now-casting in Austria, *Advances in Space Research,* 47(10), 1691–1703, https://doi.org/10.1016/j.asr.2010.10.028, 2011.

Kober, K. and Tafferner, A.: Tracking and nowcasting of convective cells using remote sensing data from radar and satellite, *Meteorologische Zeitschrift*, 1(18), 75-84, https://doi.org/10.1127/0941-2948/2009/359, 2009.

Koper, K.D. & Burlacu, R.: The fine structure of double-frequency microseisms recorded by seismometers in North America. *Journal of Geophysical Research: Solid Earth*, 120(3), 1677-1691. https://doi.org/10.1002/2014JB011820, 2015.

Landès, M., Ceranna, L., Le Pichon, A. and Matoza, R.S.: Localization of microbarom sources using the IMS infrasound network. *Journal of Geophysical Research: Atmospheres*, 117(D6), https://doi.org/10.1029/2011JD016684, 2012.

Landskron, D., Böhm, J.: VMF3/GPT3: refined discrete and empirical troposphere mapping functions, *Journal of Geodesy,* 92, 349–360, https://doi.org/10.1007/s00190-017-1066-2, 2018.

Li, L., Boué, P., Retailleau, L., & Campillo, M.: Spatiotemporal Correlation Analysis of Noise-Derived Seismic Body Waves With Ocean Wave Climate and Microseism Sources, *Geochemistry, Geophysics, Geosystems*, 21(9), https://doi.org/10.1029/2020GC009112, 2020.

Listowski, C., Forestier, E., Dafis, S., Farges, T., De Carlo, M., Grimaldi, F., Le Pichon, A., Vergoz, J., Heinrich, P. and Claud, C.: Remote monitoring of Mediterranean hurricanes using infrasound, *Remote Sensing*, 14(23), 6162, https://doi.org/10.3390/rs14236162, 2022.

MacQueen, J.: Some methods for classification and analysis of multivariate observations, in: Proceedings of the Fifth Berkeley Symposium on Mathematical Statistics and Probability, Berkeley, California, January 1967, 5, 281-298, 1967.

Marut, G., Hadas, T., Kaplon, J., Trzcina, E. and Rohm, W.: Monitoring the water vapor content at high spatio-temporal resolution using a network of low-cost multi-GNSS receivers, *IEEE Transactions on Geoscience and Remote Sensing*, 60, 1-14, https://doi.org/10.1109/TGRS.2022.3226631, 2022.

Pásztor, M., Czanik, C. and Bondár, I.: A single array approach for infrasound signal discrimination from quarry blasts via machine learning, *Remote Sensing*, 15(6), 1657, https://doi.org/10.3390/rs15061657, 2023.

Le Pichon, A., Matoza, R., Brachet, N. and Cansi, Y.: Recent enhancements of the PMCC infrasound signal detector. *Inframatics*, *26*, 5-8, 2010.

Priego, E., Jones, J., Porres, M.J. and Seco, A.: Monitoring water vapour with GNSS during a heavy rainfall event in the Spanish Mediterranean area, Geomatics, Natural Hazards and Risk, 8(2), 282–294, https://doi.org/10.1080/19475705.2016.1201150, 2017.

Retailleau, L. & Gualtieri, L.: Multi-phase seismic source imprint of tropical cyclones, *Nature Communications*, 12(1), https://doi.org/10.1038/s41467-021-22231-y, 2021.

Rindraharisaona, E.J., Réchou, A., Fontaine, F.R., Barruol, G., Stamenoff, P., Boudevillain, B., Rigaud-Louise, F. and Delcher, E.: Seismic signature of rain and wind inferred from seismic data, *Earth and Space Science*, 9(10), p.e2022EA002328, 2022.

Sokol, Z., Szturc, J., Orellana-Alvear, J., Popova, J., Jurczyk, A. and Célleri, R.: The role of weather radar in rainfall estimation and its application in meteorological and hydrological modelling—A review, *Remote Sensing*, 13(3), 351, 2021.

Stopa, J.E., Cheung, K.F., Garcés, M.A. and Badger, N.: Atmospheric infrasound from nonlinear wave interactions during Hurricanes Felicia and Neki of 2009, *Journal of Geophysical Research: Oceans*, 117(C12), https://doi.org/10.1029/2012JC008257, 2012

Stott, P.: How climate change affects extreme weather events. *Science,* 352(6293), 1517-1518, https://doi.org/10.1126/science.aaf7271, 2016.

Tanimoto, T. & Anderson, A.: Seismic noise between 0.003 Hz and 1.0 Hz and its classification, *Progress in Earth and Planetary Science*, 10(1), https://doi.org/10.1186/s40645-023-00587-7, 2023.

Vaquero-Martínez, J. and Antón, M.: Review on the role of GNSS meteorology in monitoring water vapor for atmospheric physics, *Remote Sensing*, 13(12), 2287, https://doi.org/10.3390/rs13122287, 2021.

Viticchie, B., Lekouara, M., Hungershöfer, K., Joro, S., Grandell, J., Maufrais, A., Marquez, M.J., Munro, R.: Algorithm Theoretical Basis Document (ATBD) for L2 processing of the MTG Lightning Imager data, Rapp. Tech. EUMESTAT, 6, 2020.

Wessel, P., Luis, J.F., Uieda, L.A., Scharroo, R., Wobbe, F., Smith, W.H. and Tian, D.: The generic mapping tools version 6, *Geochemistry, Geophysics, Geosystems*, *20*(11), 5556-5564, https://doi.org/10.1029/2019GC008515, 2019.

Wilgan, K., Rohm, W. and Bosy, J.: Multi-observation meteorological and GNSS data comparison with numerical weather prediction model, *Atmospheric Research*, 156, 29–42, https://doi.org/10.1016/j.atmosres.2014.12.011, 2015.